GPI-anchored proteins are directly targeted to the apical surface in fully polarized MDCK cells

Simona Paladino,[1,2] Thomas Pocard,[2] Maria Agata Catino,[1,2] and Chiara Zurzolo[1,2]

[1]Dipartimento di Biologia e Patologia Cellulare e Molecolare, CEINGE Biotecnologie Avanzate, Università degli Studi di Napoli Federico II, 80131 Napoli, Italy
[2]Unité de Trafic Membranaire et Pathogénèse, Institut Pasteur, 75724 Paris Cedex 15, France

The polarity of epithelial cells is dependent on their ability to target proteins and lipids in a directional fashion. The trans-Golgi network, the endosomal compartment, and the plasma membrane act as sorting stations for proteins and lipids. The site of intracellular sorting and pathways used for the apical delivery of glycosylphosphatidylinositol (GPI)-anchored proteins (GPI-APs) are largely unclear. Using biochemical assays and confocal and video microscopy in living cells, we show that newly synthesized GPI-APs are directly delivered to the apical surface of fully polarized Madin–Darby canine kidney cells. Impairment of basolateral membrane fusion by treatment with tannic acid does not affect the direct apical delivery of GPI-APs, but it does affect the organization of tight junctions and the integrity of the monolayer. Our data clearly demonstrate that GPI-APs are directly sorted to the apical surface without passing through the basolateral membrane. They also reinforce the hypothesis that apical sorting of GPI-APs occurs intracellularly before arrival at the plasma membrane.

Introduction

The plasma membrane of polarized epithelial cells is divided by tight junctions into apical and basolateral domains, which display different protein and lipid compositions that are required for a range of specialized functions. This asymmetric distribution is achieved by continuous sorting of newly synthesized components and their regulated internalization (Mellman, 1996; Matter, 2000). Evidence derived from biochemical and live imaging studies have shown that apical and basolateral membranes segregate into different vesicles upon exit from the TGN (Griffiths and Simons, 1986; Wandinger-Ness et al., 1990; Keller et al., 2001; Kreitzer et al., 2003), supporting the hypothesis that the TGN is the major sorting station during exocytosis of newly synthesized proteins. More recent work has shown that protein sorting could also occur in recycling endosomes (REs) after their exit from the TGN (Folsch et al., 2003; Ang et al., 2004), similar to what happens in yeast (Luo and Chang, 2000).

Intracellular sorting of newly synthesized proteins at the TGN or in REs is based upon recognition by the sorting machinery of specific apical and basolateral sorting signals (Mostov et al., 2000) that mediate their incorporation into apical and basolateral sorting vesicles (Wandinger-Ness et al., 1990; Keller et al., 2001; Rodriguez-Boulan et al., 2005). As a result of these events, proteins can be transported to the surface after either a direct or an indirect (transcytotic) route that first passes through the opposite membrane domain. Utilization of the direct or indirect pathways seems to be both cell and protein specific (Rodriguez-Boulan et al., 2005). For example, in liver cells, the majority of proteins follow an indirect pathway, whereas in Caco-2 intestinal cells, both pathways are used, and the choice is likely to be protein specific. In MDCK (kidney) and FRT (Fischer rat thyroid) cells, the direct pathway is more commonly used, whereas the transcytotic pathway seems to be more specific for basolateral proteins and transmembrane receptors (Mostov et al., 1986; Sarnataro et al., 2000), where specific signals for this route have been found (Casanova et al., 1990; Apodaca and Mostov, 1993; Song et al., 1994). In these cells, apical proteins mainly use a direct pathway (Rodriguez-Boulan et al., 2005), and the indirect pathway has been shown mainly during the establishment of the polarized epithelium (Zurzolo et al., 1992; Rodriguez-Boulan et al., 2005).

Basolateral sorting is mediated by discrete domains in the cytosolic protein tail frequently containing tyrosine or dileucine motifs (Bonifacino and Traub, 2003), which are recognized by the clathrin adaptor complex (Folsch et al., 1999; Sugimoto et al., 2002). However, the situation is more complicated for apical proteins because lumen-localized domains, transmembrane domains, and membrane-binding features have all been shown to be important for apical sorting (Scheiffele et al., 1995, 1997;

Correspondence to Chiara Zurzolo: zurzolo@pasteur.fr; zurzolo@unina.it

Abbreviations used in this paper: GPI, glycosylphosphatidylinositol; GPI-AP, GPI-anchored protein; NTR, neurotrophin receptor; PATJ, Pals1-associated tight junction protein; PLAP, placental alkaline phosphatase; RE, recycling endosome; TER, transepithelial resistance.

The online version of this article contains supplemental material.

The Journal of Cell Biology, Vol. 172, No. 7, March 27, 2006 1023–1034
http://www.jcb.org/cgi/doi/10.1083/jcb.200507116

Chuang and Sung, 1998; Sun et al., 1998; Lipardi et al., 2000). A case in point are the glycosylphosphatidylinositol (GPI)-anchored proteins (GPI-APs) that have been shown to be directly targeted to the apical domain after lateral segregation from basolateral cargo in the TGN (Keller et al., 2001) because of their incorporation into sphingolipid- and cholesterol-rich microdomains (rafts), which were assayed by their insolubility in cold detergents (Brown and Rose, 1992; Simons and Ikonen, 1997). However, it was recently demonstrated that association with detergent-resistant microdomains is not sufficient to determine apical sorting of GPI-APs but that stabilization into rafts, promoted by their oligomerization (which most likely leads to the coalescence of more rafts), is required (Paladino et al., 2004). It was also found that oligomerization of GPI-APs begins in the medial Golgi and is concomitant with association in detergent-resistant microdomains. Therefore, this data suggest that sorting of apical GPI-APs occurs during passage through the Golgi apparatus, presumably at the TGN and before reaching the plasma membrane. This hypothesis has been supported by several biochemical experiments showing that after their segregation at the TGN, GPI-APs are directly delivered from the Golgi to the apical plasma membrane (Arreaza and Brown, 1995; Lipardi et al., 2000).

The aforementioned model has been challenged recently by Polishchuk et al. (2004), who, by using state of the art technologies for imaging in living cells, have shown that a GPI-linked protein (GFP-GPI) was apically targeted after a transcytotic route, thus suggesting that apical sorting of GPI-APs occurs after membrane delivery. However, the experiments showing either direct or indirect sorting of GPI-APs in living cells have been performed in conditions that were not fully polarized because of the difficulty of imaging polarized cells growing on a filter in three dimensions and in transiently transfected cells where biochemical experiments are difficult to perform. Therefore, to understand the routing and sorting site of GPI-APs, we directly followed the sorting and trafficking of three different GPI-APs to the apical surface of stably transfected clones of MDCK cells by using both biochemical and live imaging approaches in fully polarized cells. We demonstrate that all proteins are directly delivered to the apical surface and that the impairment of basolateral fusion/endocytosis does not affect apical transport, thus suggesting that sorting occurs intracellularly before reaching the plasma membrane.

Results

Newly synthesized GPI-APs are directly targeted to the apical surface in fully polarized monolayers

The mechanism of sorting and the route that GPI-APs follow to reach the apical membrane are still debated. We have recently shown that both raft association and protein oligomerization are required for apical sorting of GPI-APs. These two events occur concomitantly in the Golgi apparatus, suggesting that the sorting of GPI-APs occurs in the Golgi (Paladino et al., 2004). In direct contrast to these data, a recent study using live imaging techniques showed that a chimeric GPI protein (GFP-GPI) is apically targeted by a transcytotic pathway in MDCK cells (Polishchuk et al., 2004).

We decided to directly investigate the pathway and the sorting site of GPI-APs by using both biochemical and imaging approaches and three different GPI model proteins stably transfected in MDCK cells: GFP-GPI, encoded by the same cDNA used in the live study of Polishchuk et al. (2004); placental alkaline phosphatase (PLAP), a native GPI-AP; and neurotrophin receptor (NTR)–PLAP, in which the ectodomain of $p75^{NTR}$ is fused to the GPI attachment signal of PLAP (Monlauzeur et al., 1998; Lipardi et al., 2000). To analyze the pathway followed by the newly synthesized GPI-APs, we performed a biotin-targeting assay (Zurzolo et al., 1992). Fully polarized MDCK cells grown on filters for 4 d were pulse labeled with [^{35}S]methionine for 15 min and chased for the indicated times (Fig. 1 A). At each chase time, biotin was added to the apical or basolateral surface to catch the arrival of the protein at the plasma membrane. After 15 min of chase, GFP-GPI was detected on the apical surface, and it progressively accumulated on this domain, whereas very low amounts also accumulated with similar kinetics on the basolateral plasma membrane (Fig. 1 A). These results suggest that GFP-GPI follows a direct route to reach the apical surface and that small amounts of the protein are missorted to the basolateral domain.

To rule out the possibility that this behavior was specific for GFP-GPI, we performed the same experiment using PLAP. Newly synthesized PLAP was initially detected on the apical surface after 60 min of chase and accumulated there for up to 2 h (Fig. 1 A). A small amount of the protein was missorted to the basolateral domain at all chase times, as was found for GFP-GPI, indicating that PLAP also followed a direct apical route. Similar results were obtained with NTR-PLAP in 4-d-old monolayers (Fig. S1 A, available at http://www.jcb.org/cgi/content/full/jcb.200507116/DC1).

It was previously shown that during the establishment of a polarized monolayer in filter culture, apical proteins that are normally sorted via a direct route can use the transcytotic pathway (Zurzolo et al., 1992). Because of this, we repeated the same targeting assay in MDCK cells grown on filter for just 1.5 d (Fig. 1 B). Also in these conditions, we found that both GFP-GPI and PLAP were directly targeted to the apical surface, although a higher amount of both proteins was missorted to the basolateral surface in comparison with the fully polarized 4-d-old cultures. Interestingly, in one case, we found that a small amount of GFP-GPI accumulated on the basolateral surface before reaching the apical membrane (Fig. S1 B), which is a classic behavior for a transcytotic protein. Thus, to establish the influence of time in culture for the initial establishment of the apical delivery of GFP-GPI, we repeated the targeting assays after 1, 2.5, and 4 d in culture. By quantifying different experiments, we could show that the basolateral delivery of GFP-GPI observed after 1 d of culture progressively disappeared over several days (Fig. 1 C) and that the apical polarity of GFP-GPI increased from 50% on the first day to 80% on the fourth day of culture (Fig. 1 C). These results confirmed our previous findings that an indirect route could be used during the establishment of a polarized monolayer to salvage missorted proteins and

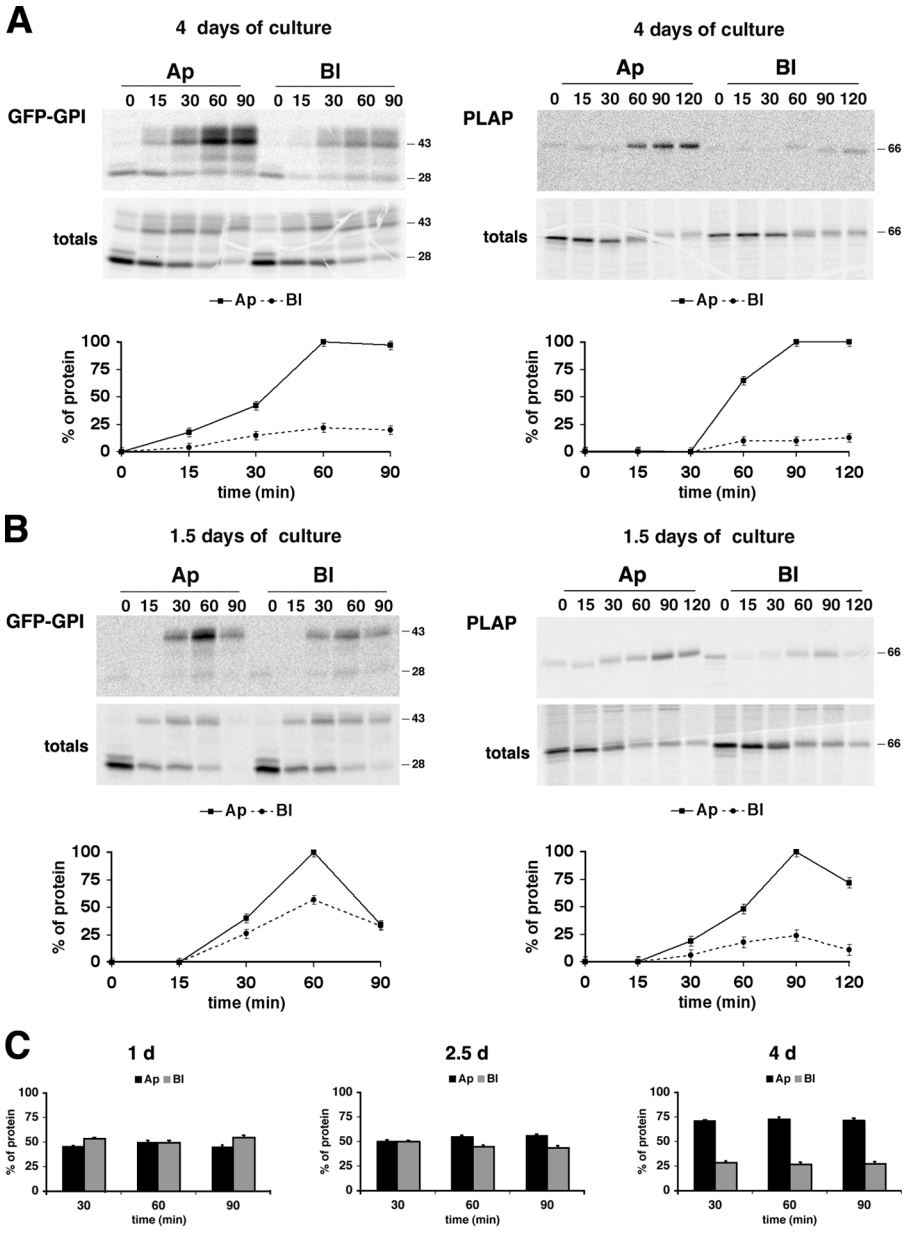

Figure 1. **Newly synthesized GPI-APs are directly targeted to the apical surface.** MDCK cells stably expressing GFP-GPI or PLAP grown on filters for 4 (A) or 1.5 d (B) were pulsed for 15 min with [^{35}S]methionine and chased for the indicated times. At the end of each chase time, cells were labeled with LC-biotin and added to the apical (Ap) or basolateral (Bl) surface, respectively. Cell lysates were immunoprecipitated with specific antibodies. The biotinylated proteins were recovered from the immunoprecipitates by reprecipitation with streptavidin beads. After running on SDS-PAGE, samples were analyzed by phosphorimager. One tenth of immunoprecipitates (totals) was kept before streptavidin precipitation and shown in the bottom panels. The monomer form of GFP-GPI (28 kD) and the slower mobility band (43 kD), a partially denaturated GFP dimer that was previously described (Inouye and Tsuji, 1994; Paladino et al., 2004), are indicated. Fluorograms of four different experiments were quantified, and the results were expressed as a percentage of the amount at the time of maximal surface expression. For GFP-GPI, the quantification is referred to as the upper and lower bands together. (C) MDCK cells stably expressing GFP-GPI grown on filters for 1, 2.5, and 4 d were pulsed for 15 min with [^{35}S]methionine, chased for 30, 60, and 90 min, and processed as in A and B. Results from four different experiments were plotted as percent apical and basolateral surface expression. Error bars represent SD.

reestablish the correct polarity (Zurzolo et al., 1992). This behavior appears to be protein specific (Rodriguez-Boulan et al., 2005) because it was observed for GFP-GPI and NTR-PLAP (Fig. S1, A and B) but never for PLAP.

GFP-GPI accumulated in the Golgi is also targeted directly to the apical surface

The biotin-targeting assay analyzes only newly synthesized proteins. Because it has been shown that GPI-APs can recycle intracellularly through the Golgi apparatus (Nichols et al., 2001), it is possible that the newly synthesized and recycled proteins follow different pathways and that their sorting sites are, therefore, different. To analyze exclusively the targeting of GPI-APs from the Golgi apparatus, we set up a cold targeting assay using a Golgi temperature block combined with protease digestion.

To eliminate the protein already present on the plasma membrane, 25 μg/ml trypsin was added for 1 h to the apical and basolateral sides of filter-grown MDCK cells expressing GFP-GPI. This treatment was able to remove almost all GFP-GPI present at steady state on the surface (Fig. S2, A and B; available at http://www.jcb.org/cgi/content/full/jcb.200507116/DC1). Conversely, by confocal microscopy, we did not detect any GFP signal on the surface to which the enzyme was added (Fig. S2 A). By Western blotting, we found the protein only in the media of trypsin-treated cells (Fig. S2 B), thus indicating that trypsin does not pass trough the monolayer but digests only the proteins present on the side exposed to it (Fig. S2, A and B).

After clearing the surface by trypsin treatment, fully polarized monolayers were subjected to a temperature block by incubation at 19.5°C in the presence of cycloheximide to accumulate the protein in the Golgi and to eliminate newly

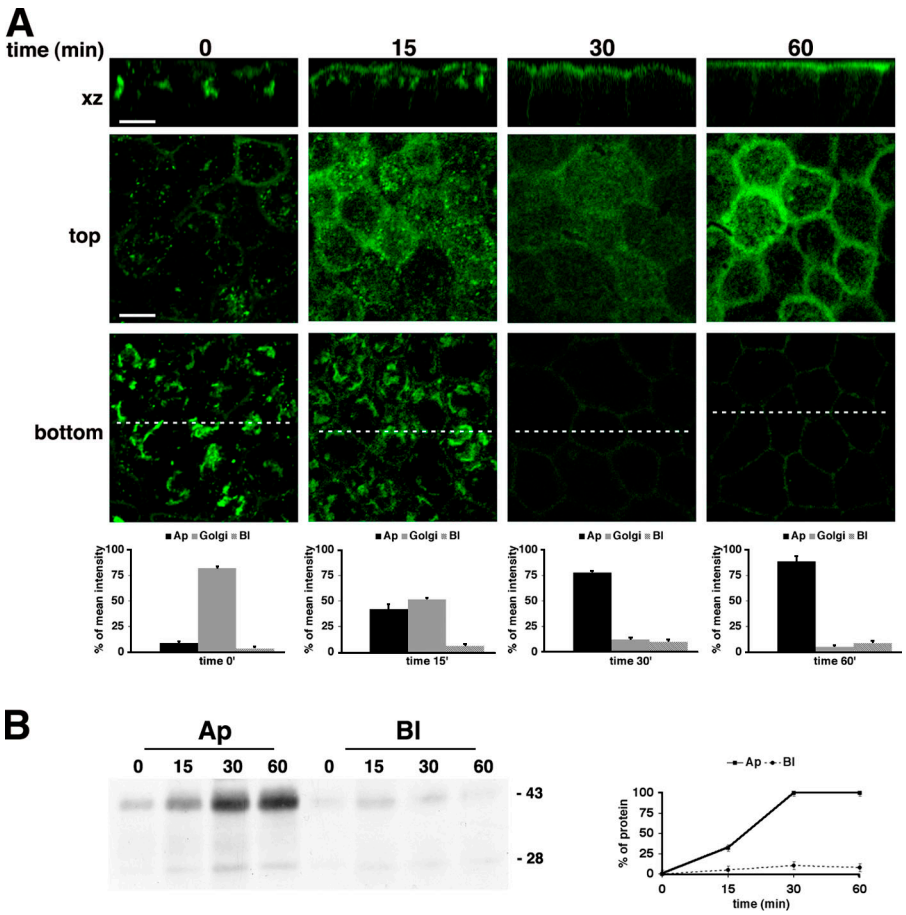

Figure 2. **GFP-GPI is directly delivered from the Golgi to the apical surface.** MDCK cells stably expressing GFP-GPI grown on filter for 4 d were incubated with trypsin to eliminate all proteins at the surface and were subjected to a temperature block to accumulate proteins in the TGN (see Materials and methods). Cells were then warmed at 37°C for the indicated times in culture medium containing cycloheximide. After each time point, cells were fixed and treated for confocal microscopy where serial confocal sections were collected from the top to the bottom of the cell monolayer (A). The dashed lines show the positions from where the xz sections were taken. Mean fluorescence intensities at the Golgi, apical, and basolateral domains were measured at the different chase times and expressed as percentages of total fluorescence (A, bottom; see Materials and methods). Alternatively, cells were biotinylated from the apical (Ap) or basolateral (Bl) side. After lysis, GFP-GPI was immunoprecipitated with an antibody against GFP and revealed by using HRP-streptavidin (B). Gels from three different experiments were quantified, and the results were expressed as percentages of the amount at the time of maximal surface expression. The amount of protein still present at the apical or basolateral surface at time = 0 was subtracted from all chase times. Error bars represent SD. Bars, 10 μm.

synthesized proteins. Cells were then warmed at 37°C for the different indicated times in the presence of cycloheximide, and the arrival of proteins at the cell surface was assayed both by confocal microscopy (Fig. 2 A) and by domain-selective biotinylation at different chase times (Fig. 2 B). For microscopy, cells were fixed and imaged by collecting z axis stacks to visualize all of the protein inside the cells. Xz reconstructions are shown for different times in Fig. 2 A. At time = 0, GFP-GPI was present almost exclusively in the Golgi apparatus, as was previously demonstrated (Keller et al., 2001; Paladino et al., 2004; Polishchuk et al., 2004). The ring sometimes observed at the top of the cells at time = 0 in the xy section (also see Figs. 5 and 7) represents the edge of the apical surface, possibly as a result of incomplete trypsin digestion. During the chase times, GFP-GPI progressively accumulated on the apical surface, as clearly shown both in xz microscopy sections and in xy sections collected from the top of the cells as well as by quantification of the fluorescent signal in selected regions from a single z plane at different heights through the cell (Fig. 2 A). Consistent with the confocal data, we found by surface biotinylation that after 15 min at 37°C, GFP-GPI began to arrive at the apical surface and accumulated there for up to 60 min (Fig. 2 B). Thus, both these approaches confirmed that GFP-GPI previously accumulated in the Golgi is directly targeted to the apical surface.

Exposure of the basolateral membrane to tannic acid or trypsin does not affect the apical arrival of GFP-GPI

To rule out the possibility that we were missing a fast passage of proteins through the basolateral surface, we used two approaches. In one, we added trypsin to the basolateral surface to remove any protein that was passing through the basolateral domain, and, in the other, we inhibited basolateral traffic using tannic acid as previously described (Polishchuk et al., 2004).

In the first approach, to detect proteins passing through the basolateral surface, we adapted an assay that was used before to demonstrate transcytosis of the polymeric Ig receptor in MDCK cells (Casanova et al., 1990). We added 25 μg/ml trypsin to the basolateral medium during the chase time course at 37°C after the temperature block so that the molecules passing through the basolateral surface would be proteolysed and should not be recovered at the apical surface. To the contrary, molecules directly delivered to the apical surface would not be exposed to trypsin and would be detected normally. In the presence of trypsin, GFP-GPI was still apically delivered to the same extent as in untreated cells (Fig. 3), and only the portion of protein that was missorted to the basolateral surface was recovered in the basolateral media as a faster migrating, partially digested form (Fig. 3). It is to be expected that the β barrel of GFP will be more resistant to enzymatic activity, whereas the loops outside the barrel would be digested. On the other hand,

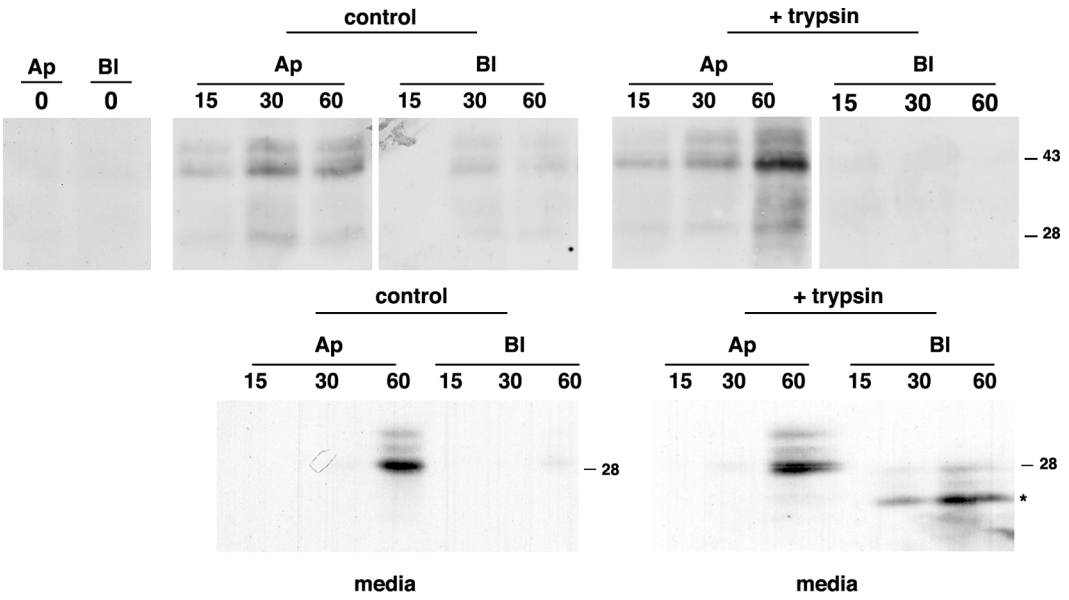

Figure 3. **GFP-GPI still reaches the apical surface in the presence of trypsin in the basolateral medium.** MDCK cells stably expressing GFP-GPI grown on filter for 4 d were incubated with trypsin, subjected to a temperature block in the TGN (see Materials and methods), and chased at 37°C for the indicated times (in minutes) in the presence or absence of 25 μg/ml trypsin in the basolateral media. After each chase time, cells were selectively biotinylated from the apical (Ap) or basolateral (Bl) surface. After immunoprecipitation with an antibody against GFP, samples were run on SDS-PAGE and revealed using HRP-streptavidin. Apical and basolateral media for control and treated cells were recovered at all chase times, proteins were TCA precipitated, run on SDS-PAGE, and revealed by Western blotting using GFP antibody. The asterisk indicates the trypsin partially digested form of GFP-GPI.

the GFP-GPI that was detected in the apical media after 60 min of chase time both in control and in treated cells likely represents the proportion of protein that is normally shedded from the cell surface, and it runs on the gel at its expected molecular weight. These experiments further confirm that GFP-GPI does not need to travel through the basolateral surface before reaching the apical plasma membrane.

As an alternative to trypsin, we used tannic acid, a cell-impermeable fixative that cross-links cell surface carbohydrate groups and does not diffuse across tight junctions (Newman et al., 1996; Polishchuk et al., 2004). When added selectively to the different domains of the plasma membrane of filter-grown cells, tannic acid would be expected to inhibit plasma membrane fusion and internalization only in the specific domain to which it was added. To check whether the tannic acid impairs internalization in MDCK cells, we followed transferrin endocytosis (Fig. S3, available at http://www.jcb.org/cgi/content/full/jcb.200507116/DC1). In control cells, transferrin was exclusively localized in intracellular spots, whereas in cells treated with tannic acid, it was blocked at the cell surface after 30 min of internalization (Fig. S3, top). We also show that tannic acid does not affect binding but only affects the internalization of transferrin by allowing first its binding for 5 min at 37°C and then the internalization for 30 min in the presence or absence of basolateral tannic acid (Fig. S3, bottom). Also in this case, in the presence of tannic acid, transferrin was exclusively found at the basolateral membrane. Furthermore, these results showed that a pretreatment with tannic acid for 30 min impairs plasma membrane internalization at least for the next 30 min. Thus, it appeared to be a convenient tool to analyze whether a protein follows a transcytotic pathway via the basolateral surface because this process requires the protein to first be endocytosed (Polishchuk et al., 2004).

To analyze the effect of tannic acid on GFP-GPI trafficking, we repeated the same cold targeting assay as described in Fig. 2. After the trypsin treatment, cells grown for 4 d on filters were incubated at 19.5°C in the presence of cycloheximide for 2 h to accumulate the protein in the Golgi. During the last 30 min at 19.5°C, 0.5% tannic acid was added to the basolateral medium to block basolateral fusion. After washing to remove tannic acid, the monolayers were then incubated at 37°C in the presence of cycloheximide for the different indicated times to follow the arrival of the protein at the surface (Fig. 4, A and B). We found both by confocal microscopy (Fig. 4 A) and by surface biotinylation (Fig. 4 B) that in the presence of tannic acid, GFP-GPI still reached the apical surface directly with similar kinetics to the untreated cells (Fig. 2, A and B). However, by confocal microscopy, it appears that in tannic acid–treated cells, trafficking of the protein is slightly slower, and the newly arrived protein appears to fuse or accumulates mainly at the edge of the apical surface above the tight junctions. Unexpectedly, a small portion of GFP-GPI was detected on the bottom confocal sections or by biotinylation of the basolateral surface. This basolateral signal could result either from the fusion of some GFP-GPI–containing carriers with the basolateral surface or from diffusion of the protein from the apical domain, therefore implying either an incomplete effect of tannic acid in blocking basolateral fusion or an effect of tannic acid on the integrity of the tight junctions. Nonetheless, both the tannic acid and the trypsin experiments showed that GFP-GPI does not need to reach the basolateral surface to be apically sorted but is directly targeted to the apical membrane.

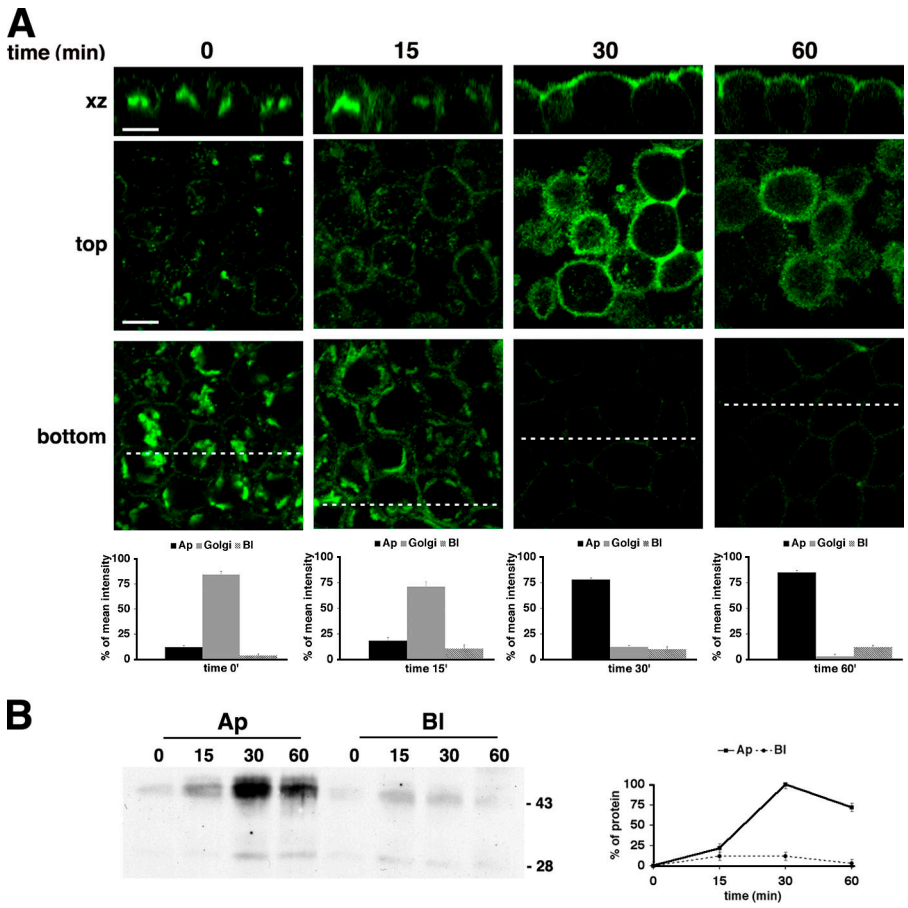

Figure 4. **Tannic acid does not affect the apical targeting of GFP-GPI.** MDCK cells stably expressing GFP-GPI grown on filter were incubated with trypsin and subjected to a temperature block in the TGN (see Materials and methods). Tannic acid was added to the basolateral medium 30 min before release from the 20°C block. Cells were then warmed at 37°C for the indicated times in the absence of tannic acid in culture medium containing cycloheximide. After each time point, cells were fixed and quenched. Serial confocal sections were collected from the top to the bottom of cell monolayers (A). The dashed lines show the positions from where the xz sections were taken. Mean fluorescence intensities at the Golgi, apical (Ap), and basolateral (Bl) domains were measured as in Fig. 2. Alternatively, surface proteins were biotinylated from the apical or basolateral side, immunoprecipitated with GFP antibody, and revealed by using HRP-streptavidin (B). Results from three different experiments were plotted as the percentage of the amount at the time of maximal surface expression. The value at the apical or basolateral surface at time = 0 was subtracted from all chase times. Error bars represent SD. Bars, 10 μm.

Long-term incubation with tannic acid alters the integrity of fully polarized monolayers and causes the mislocalization of GFP-GPI

We reasoned that if the low level of basolateral missorting observed in the aforementioned experiments was caused by an initial effect of tannic acid on the integrity of the monolayer, it should increase with the time of the treatment. Therefore, we incubated cells grown on filter for 4 d with basolateral tannic acid during the last 10 min of the temperature block and during all chase times at 37°C as shown previously by Polishchuk et al. (2004). The cells were then fixed and imaged by confocal microscopy or subjected to surface biotinylation (Fig. 5). Also in this case, at time = 0, GFP-GPI is present in the Golgi apparatus. However, after 30 min of chase, it is present both on the apical and on the basolateral surface and continues to be completely mislocalized after 60 min (Fig. 5 A). These results were confirmed by the surface biotinylation assay that showed a complete mislocalization of the protein (Fig. 5 B). These data suggest that a long treatment with tannic acid leads to monolayer depolarization.

To address whether tannic acid could alter the integrity of the cell monolayer, we evaluated the functional state of tight junctions during tannic acid treatment by different methods (Matter and Balda, 2003). First, we investigated the morphology of the tight junctions by staining them with an antibody against PATJ (Pals1-associated tight junction protein), a component of tight junctions (Lemmers et al., 2002; Shin et al., 2005). To verify that the basolateral domain maintains its physical integrity, we labeled the cells with an antibody against Na,K-ATPase (Fig. 6 A). In control cells, PATJ staining results in a chicken wire–like pattern (typical of tight junction markers) that was detected exclusively in one z plane (at 2.5 μm from the out-of-focus top signal) where the signal for the Na,K-ATPase was almost completely out of focus. On the other hand, a distinct signal for Na,K-ATPase was detectable starting at 6.5 μm from the top out-of-focus signal all along the lateral membrane (Gottardi and Caplan, 1993; Zurzolo and Rodriguez-Boulan, 1993). In contrast, in cells treated with tannic acid, the PATJ signal was found also in the bottom planes at the same level where the Na,K-ATPase–derived signal was in focus. This effect was more evident after 60 min of treatment. These results indicated that tight junctions were impaired by tannic acid treatment. To then check the integrity of the monolayers, we measured both the passage of electric current and the flux of a tracer across monolayers, which are the two most commonly used methods to analyze the integrity of tight junctions (Matter and Balda, 2003).

Transepithelial resistance (TER) of fully polarized monolayers was measured before and after basolateral incubation with tannic acid for 30–60 min. Although in control cells TER is stable during the time course of the measurements, in treated cells, it decreased progressively (Fig. 6 B). After 60 min of tannic acid treatment, the TER decreased to the value of empty filters.

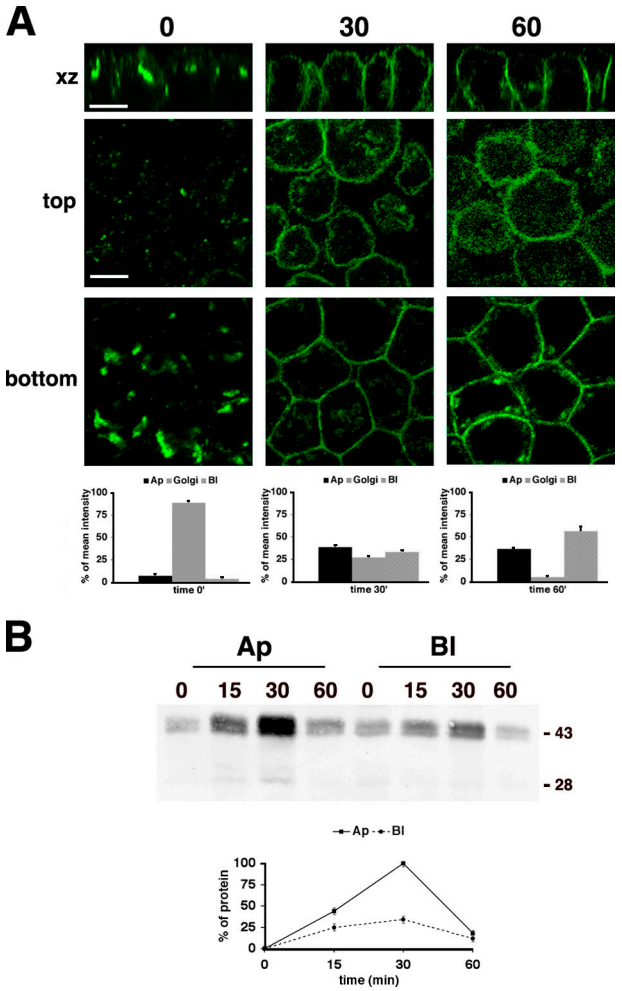

Figure 5. **Long tannic acid treatment leads to the depolarization of GFP-GPI.** MDCK cells stably expressing GFP-GPI grown on filter were incubated with trypsin and subjected to a temperature block in the TGN. Tannic acid was added to the basolateral medium 10 min before release from the 20°C block. Cells were warmed at 37°C for the indicated times in culture medium containing cycloheximide in the presence of tannic acid. After each time point, cells were fixed, quenched, and analyzed by confocal microscopy. Mean fluorescence intensities at the Golgi, apical (Ap), and basolateral (Bl) domains were measured as in Fig. 2. Alternatively, surface proteins were biotinylated from the apical or the basolateral side, immunoprecipitated with GFP antibody, and revealed by using HRP-streptavidin (B). Results from three different experiments were plotted as percentages of the amount at the time of maximal surface expression. The value at the apical or basolateral surface at time = 0 was subtracted from all chase times. Error bars represent SD. Bars, 10 μm.

Finally, we performed a permeability assay using [^{14}C]inulin as previously described (Apodaca et al., 1995). Cells grown on filter for 4 d were treated with tannic acid on the basolateral side for 30 or 60 min. At the same time, [^{14}C]inulin (1 μCi per filter) was added to the apical medium. Subsequently, apical and basolateral media were recovered, and C^{14} was quantified. The extent of inulin passage was quantified by dividing the amount of [^{14}C]inulin found in the basal chamber by the total [^{14}C]inulin added to each sample. We found that in the control cell monolayer, only 0.25 ± 0.01% and 0.49 ± 0.03% of apically added [^{14}C]inulin for 30 or 60 min, respectively, was found in the basal well, whereas in the cells treated for the same length of time with basolateral tannic acid, 1.2 ± 0.01% and 3.75 ± 0.09% was collected after 30 and 60 min, respectively (Fig. 6 C). These results clearly show that the permeability of the cell monolayer is strongly altered by tannic acid treatment in a time-dependent manner (fivefold more after 30 min and eightfold more after 60 min). Thus, the nonpolarized targeting results shown in Fig. 5 (A and B) are explained by the fact that after long tannic acid treatment, although the intracellular sorting might still occur, the polarity is lost because tight junctions are impaired and the monolayer permeability is altered, thus allowing both apical/basolateral protein diffusion and passage of the biotin between the apical and basolateral compartments.

Monitoring of GFP-GPI apical targeting in living, fully polarized filter-grown cells

Although the aforementioned confocal and biochemical experiments clearly showed a direct apical arrival of GFP-GPI, they represent images taken at specific times of chase corresponding to times used in the biochemical assays. The most direct method to analyze the targeting pathway of GPI-APs would be to follow the route of GFP-GPI all the way from the Golgi to the surface in living cells using an imaging approach. This has never been possible before in fully polarized cells grown on filters because of the limits of the imaging systems for acquisition along the z axis, so all the dynamic studies on protein sorting to date have been performed in cells grown on coverslips in semipolarized conditions (Jacob and Naim, 2001; Keller et al., 2001; Jacob et al., 2003; Polishchuk et al., 2004). We used a confocal imaging system based on spinning disc technology that has the advantage of being faster and causes less photobleaching in comparison with laser scanning–based confocal methods. This system has been previously used to follow apical and basolateral cargos for short times in cells grown to confluency on coverslips (Kreitzer et al., 2003), whereas we have used it to monitor the arrival of GFP-GPI from the Golgi to the plasma membrane in live cells grown on filters in fully polarized conditions (Fig. 7). After incubation at 19.5°C, cells grown on filters were warmed at 37°C on the microscope stage, and images were taken every 3 min for a total of 60 min (Fig. 7 A). For each time point, an average of 20 z planes were collected to detect the signal from the whole cell volume. In Fig. 7 A, selected frames of the time lapse show a gradual brightening only of the apical surface as a result of GFP-GPI arrival both in control and tannic acid–treated cells. However, from the side view images (Fig. 7 A, bottom), it is possible to note an extension of the fluorescent signal toward the lateral side of the cells in the presence of tannic acid. Videos 1 and 2 (for control and treated cells, respectively; available at http://www.jcb.org/cgi/content/full/jcb.200507116/DC1) obtained after volume rendering clearly showed that the fluorescent signal of GFP-GPI, which is present at the beginning of the experiment at the TGN, gradually brightened the apical surface, whereas no transient brightening was observed at the basolateral surface (as indicated by rotation of the entire cell monolayer). Furthermore, Videos 3 and 4 (for control and treated cells, respectively) mounted with a rotation of 45° with respect to the z axis showed clearly that the signal reached the apical surface progressively, which was well defined by its typical dome aspect.

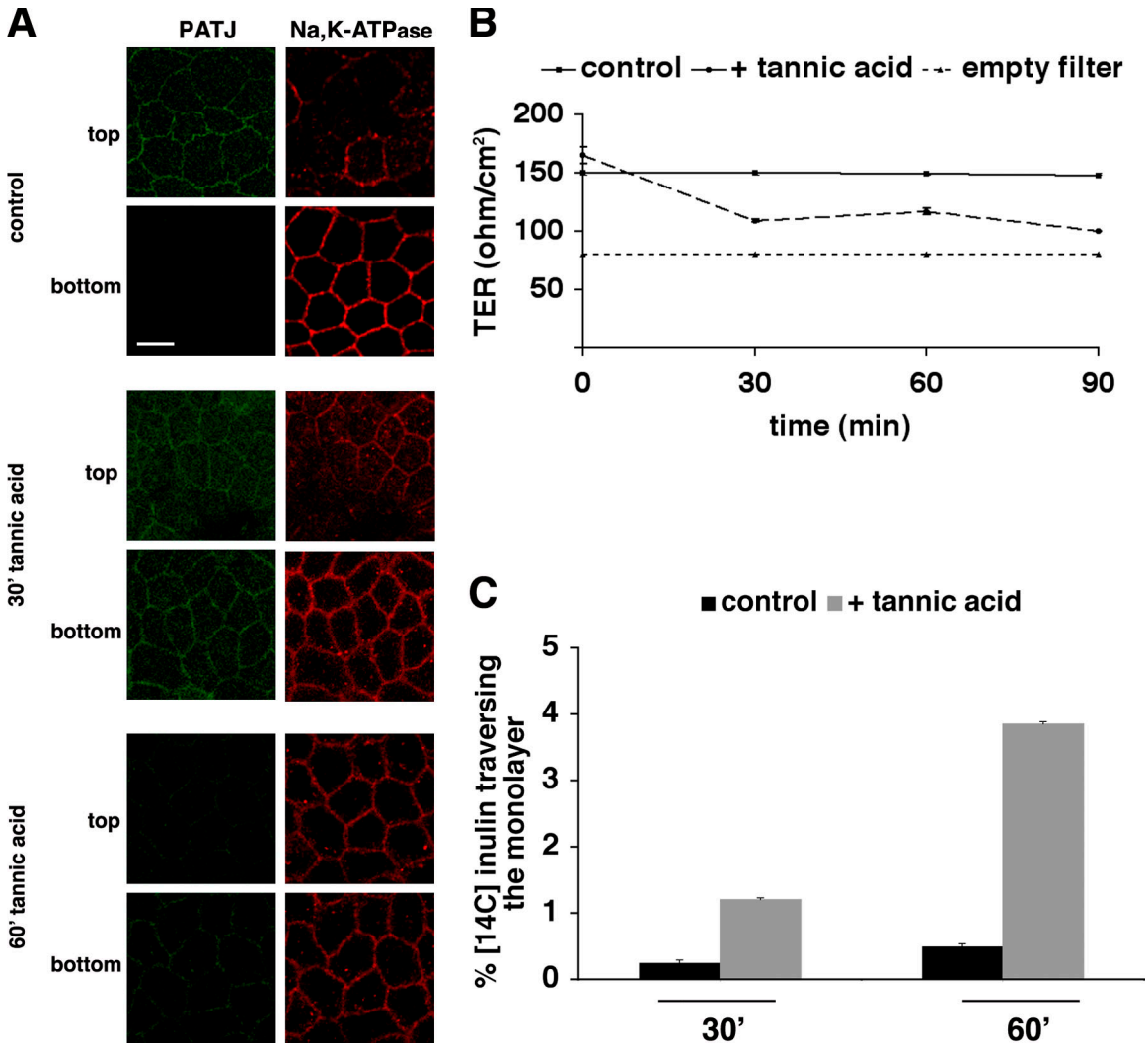

Figure 6. **Long tannic acid treatment alters the tight junctions and affects the integrity of the monolayer.** Tannic acid was added to MDCK cells grown on filters for 30 or 60 min at 37°C. (A) Cells were then fixed and stained with specific antibodies against PATJ (green) and Na,K-ATPase (red) in permeabilized conditions. Serial confocal sections were collected from the top to the bottom of cell monolayers. (B) After culturing MDCK cells on filter for 4 d, media were replaced, and transepithelial resistance (TER) was measured periodically over 90 min in the absence (control) or presence of tannic acid added to the basolateral side. (C) [^{14}C]inulin was added to the apical medium of MDCK cells grown on filter, whereas tannic acid was added (or not; control) to the basolateral medium for the indicated times at 37°C. The permeability of the monolayers was subsequently assessed by quantitating the percentage of apical [^{14}C]inulin found in the basal well. The data are means ± SD (error bars) of three experiments. Bar, 10 μm.

Finally, by observing the cells from the top (Videos 5 and 6 for control and treated cells, respectively), the progressive accumulation over time of GFP-GPI exclusively on the top of the cell was particularly evident. A better resolution was obtained by collecting three-dimensional stacks every 60 s, thereby reducing the possibility of missing a rapid passage through the basolateral surface (Fig. 7 B and Videos 7 and 8). Furthermore, to avoid both the light absorption and the background from the filter, we seeded cells on filters upside down. In these growing conditions, GP114 and Na,K-ATPase, which are endogenous apical and basolateral markers, respectively, are correctly localized as shown by immunofluorescence (Fig. S4 A), indicating that cells were well polarized.

To monitor the arrival of GFP-GPI at the surface, we had to take images every 1 or 3 min for up to 60 min at low magnification, which did not allow the direct visualization of post Golgi carriers. To visualize the trafficking of GFP-GPI–containing carriers in cells grown on filters, we imaged the cells every 2–3 s for short time intervals (3–5 min) at high magnification. A range of 4–6 μm in depth of the cell from the bottom to the top of the Golgi apparatus was collected every 2–3 s. The time lapses showed GFP-GPI–containing membranes budding from the Golgi complex as tubular processes and post-Golgi intermediates moving toward the surface (Video 9, available at http://www.jcb.org/cgi/content/full/jcb.200507116/DC1). These three-dimensional images were comparable in resolution with the ones taken before in single plane in nonpolarized cells (Keller et al., 2001; Polishchuk et al., 2004).

To determine the site of segregation of apical and basolateral cargos, we transiently cotransfected the CFP and YFP variants of GFP-GPI and GFP-PIT (a fusion construct between the transmembrane and cytosolic domains of the low density

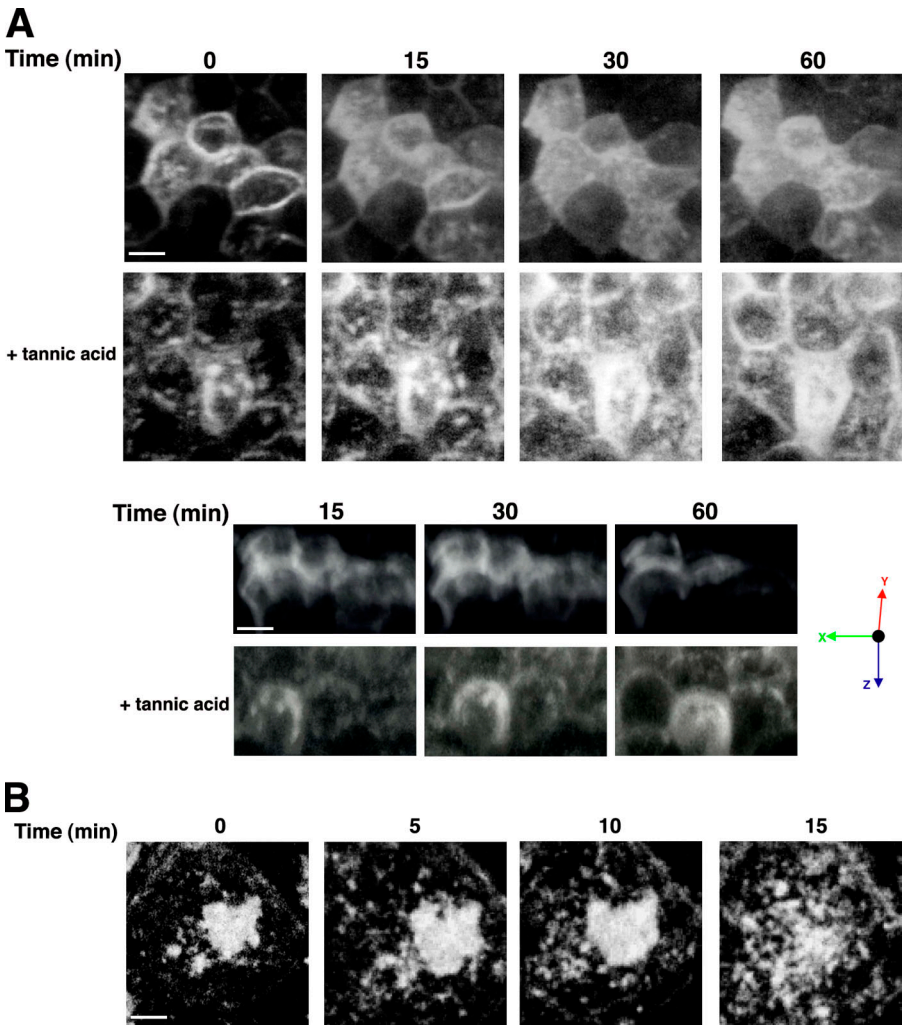

Figure 7. **GFP-GPI is directly delivered to the apical surface in living MDCK cells both in the presence and absence of tannic acid.** MDCK cells stably expressing GFP-GPI were treated as in Figs. 2 and 4. After the temperature block, cells were shifted at 37°C on the microscope and imaged live every 3 min for 60 min (A) or every 1 min for 15 min (B; also see Videos 1–8, available at http://www.jcb.org/cgi/content/full/jcb.200507116/DC1). Some frames of the time lapses three-dimensionally reconstructed with different orientations (A [top] and B, view from the apical side; A [bottom], view from the lateral side) are shown. Bars, 10 μm.

lipoprotein receptor and GFP, which is basolaterally localized as shown in Fig. S4 B), respectively. As previously described (Keller et al., 2001; Kreitzer et al., 2003; Polishchuk et al., 2004), we also found that GFP-GPI is partially segregated from a basolateral protein (YFP-PIT) in the TGN (Fig. S4 C, top) and that these proteins appear to be in distinct carriers after 10 min of release of the block (Fig. S4 C, bottom). Thus, our data demonstrate that in fully polarized monolayers, the apical delivery of GPI-APs occurs via a direct pathway, and it supports the notion that their sorting occurs intracellularly before arrival at the plasma membrane.

Discussion

Several studies have shown that apical and basolateral proteins segregate into different vesicles upon exit from the TGN (Wandinger-Ness et al., 1990; Keller et al., 2001; Kreitzer et al., 2003). GPI-APs are delivered to the apical membrane via a raft-mediated mechanism (Arreaza and Brown, 1995; Lipardi et al., 2000) and have been thought to be sorted in the TGN (Mayor and Riezman, 2004). Imaging studies in living cells have shown that GPI-APs segregate from basolateral proteins in separate carriers in the TGN, and, from there, they reach the apical surface directly (Keller et al., 2001).

Notwithstanding, a recent study based on imaging in living cells of one GPI protein (GFP-GPI) has proposed a mechanism whereby GPI-APs may use a transcytotic route to the apical surface of MDCK cells and, therefore, that their sorting occurs after arrival to the basolateral plasma membrane (Polishchuk et al., 2004). These data are in direct contrast with our model of the mechanism of GPI-AP sorting, which is based on segregation and stabilization of GPI-APs in rafts at the level of the Golgi apparatus. We believe that these two events would lead to the budding of an apical carrier that excludes basolateral proteins (Paladino et al., 2004). Because Polishchuk et al. (2004) also observed a physical segregation of the apical and basolateral cargo in the TGN, the question arises as to why this segregation would occur in regions of the Golgi membrane if the proteins are transported in the same carrier to the basolateral surface where sorting would then occur.

We directly investigated the pathway followed by three different GPI-APs to the apical surface in MDCK cells both by biochemical and imaging approaches in fully polarized cells that were grown on filters for 4 d. By using pulse-chase experiments combined with selective surface biotinylation, we found that newly synthesized proteins, PLAP, GFP-GPI, and NTR-PLAP progressively reach the apical plasma membrane without

passing through the basolateral surface (Figs. 1 and S1 A). Indeed, we never observed accumulation on the basolateral surface before the apical appearance of these proteins. We obtained the same results when we examined GFP-GPI transport to the surface that previously accumulated in the TGN after a temperature block (Figs. 2 and 7). Furthermore, by using a spinning disc confocal-based instrument, we could analyze the arrival of GFP-GPI from the Golgi to the surface in living cells grown on filters (Fig. 7 and Videos 1–9). This was not previously possible because of the thickness of polarized monolayers and the speed and sensitivity of commercially available imaging systems. The results obtained by the biochemical and imaging methods concordantly demonstrate that both newly synthesized and recycled GPI-APs are directly delivered from the TGN to the apical surface, suggesting that they are sorted intracellularly. These results were confirmed by the fact that neither basolateral cleavage by trypsin (Fig. 3) nor addition to the basolateral domain of tannic acid (Fig. 4), which inhibits basolateral transferrin endocytosis (Fig. S3), affect the apical delivery of GFP-GPI. This demonstrates that we did not miss any rapid or transient passage through the basolateral surface that could have been undetectable in the less sensitive biotinylation-based targeting assays.

The discrepancy between the results of Polishchuk et al. (2004) and our own most likely lies in the cell culture conditions and in the different methods used. The Polishchuk et al. (2004) experiments were performed in MDCK cells grown on filters for only 2–3 d, when the cells are not, in fact, fully polarized. When we performed our experiments in similar nonpolarized conditions, we found that both GFP-GPI and PLAP were missorted to the basolateral surface (Fig. 1 B) and that this missorting decreased with the time the cells were in culture (Fig. 1 C). Interestingly, in one experiment after 1.5 d in culture, we observed a transient peak of GFP-GPI at the basolateral surface before it was apically delivered (Fig. S1 B), which might suggest that it uses a transcytotic pathway in semipolarized conditions. However, as previously demonstrated, the transitory use of the transcytotic pathway appears to be a protein-specific feature (Zurzolo et al., 1992), and, in this specific case, it was observed only for GFP-GPI and for NTR-PLAP (Fig. S1 A) but not for PLAP. In addition, we demonstrate that 30 min of tannic acid is sufficient to block transferrin internalization, but it does not impair the direct apical delivery of GFP-GPI from the TGN in fully polarized cells (Fig. 4). However, when we used the same conditions as Polishchuk et al. (2004), who treated the cells with tannic acid for a longer time period (45–60 min treatment), we found that GFP-GPI becomes progressively depolarized (Fig. 5). Indeed, a prolonged treatment with tannic acid causes a redistribution of tight junction proteins and alters the integrity of the monolayer (Fig. 6), thus permitting protein diffusion from one domain to the other. Strangely enough, Polishchuk et al. (2004) did not report a basolateral GFP-GPI signal but described only accumulation in intracellular compartments. In some cells, we also observed some intracellular patches below the plasma membrane, as they described (Fig. 5, bottom; 60 min), but never saw an impairment of apical delivery (Figs. 4 and 7 and Videos 1–8). This difference could derive from the fact that they used transiently expressing cells, whereas we have used stable clones. It is well known that transiently transfected cells overexpress proteins, and overexpression is known to saturate the sorting mechanisms and to lead to missorting or the use of different pathways not used by the cells in normal conditions (Marmorstein et al., 2000).

Because, in our hands, apical surface delivery of GFP-GPI occurs rapidly (apical GFP-GPI was detected as early as 15 min after warming cells at 37°C after temperature block; Figs. 2 and 7), it is unlikely that the transcytotic route determines its steady-state distribution. In hepatocyte 5′ nucleotidase, a GPI protein following a transcytotic route to the apical surface requires 3.5 h to reach steady-state apical distribution, and this rate of transcytosis is much slower than that observed for transmembrane proteins (Schell et al., 1992). GPI-APs are slowly endocytosed from both sides (Lisanti et al., 1990; Keller et al., 1992), and they also recycle back to the surface three- to fourfold slower than other recycling membrane components (Chatterjee et al., 2001; Mayor and Riezman, 2004). Furthermore, Polishchuk et al. (2004) also found that YFP-GPI needs 2 h to be transcytosed from the basolateral side. Therefore, this discrepancy in the timing of kinetics of the arrival to the surface and the transcytotic process is inconsistent with the fact that the basolateral fraction of GPI-APs is a precursor to the apical pool. We directly ruled out this possibility by measuring the amount of missorted basolateral GFP-GPI that was internalized from the basolateral membrane in 1.5-d-old monolayers. In these conditions, a small portion (~6–8%) of GFP-GPI appeared inside the cells after 30 min of internalization at 37°C (Fig. S5, available at http://www.jcb.org/cgi/content/full/jcb.200507116/DC1), suggesting a slow internalization rate inconsistent with the use of a transcytotic pathway. However, in agreement with previous data (Zurzolo et al. 1992), this experiment also showed that some of the protein that missorted to the basolateral membrane in cells that were not fully polarized can reach the apical surface via a transcytotic pathway, as we observed the appearance of GFP-GPI at the apical surface 60 and 120 min after internalization (Fig. S5).

Our data also support the model that sorting of GPI-AP occurs intracellularly. We have recently proposed that GPI-AP oligomerization or clustering in high molecular weight complexes is the prime mechanism determining the apical sorting of GPI-APs (Paladino et al., 2004). This is because it leads to the stabilization of proteins into rafts and to the coalescence of more rafts with the consequent formation of larger functional rafts, which provide the platform for the budding of an apical carrier. Oligomerization of GPI-APs begins in the medial Golgi and is concomitant with raft association (Paladino et al., 2004), therefore supporting the hypothesis that apical GPI-AP sorting occurs at the TGN. In this study, we show that segregation between GFP-GPI and a basolateral marker (GFP-PIT) occurs during the block in the TGN and that the two proteins appear in distinct carriers after 10 min of chase at 37°C. Nonetheless, we cannot exclude the possibility that GPI-APs require travel through some endosomal compartments before reaching the apical membrane. Recently, it has been found that the inactivation of REs affect the transport of VSV-G and of an apically targeted mutant from the Golgi to the plasma membrane, suggesting

a role of REs for polarized sorting in endocytic and secretory pathways (Ang et al., 2004).

A presurface post-Golgi compartment could act as a main sorting station or as a second step after sorting at the TGN. Alternatively, it could be a pathway of salvage in the case of partial polarity or of saturation of the normal sorting machinery. For basolateral proteins, it has indeed been shown that the same sorting signals function at the level of the TGN and REs. Further studies focused and optimized to visualize the trafficking between these compartments in fully polarized cells are necessary to elucidate these different possibilities.

Materials and methods

Reagents and antibodies

Cell culture reagents were purchased from Invitrogen. Antibodies were purchased from the following companies: polyclonal anti-GFP from CLONTECH Laboratories, Inc.; monoclonal anti-GFP and Cy-5 transferrin from Invitrogen; anti-PLAP from Rockland Biosciences; and anti–Na, K-ATPase from Upstate Biotechnology. The antibodies against PATJ, GP114, and $p75^{NTR}$ were gifts from A. le Bivic (Faculté des Sciences de Luminy, Marseille, France). Biotin and streptavidin beads were obtained from Pierce Chemical Co. HRP-linked antibodies and streptavidin were purchased from GE Healthcare. All other reagents were purchased from Sigma-Aldrich.

Cell culture and transfections

MDCK cells were grown in DME containing 5% FBS. Stable clones expressing GFP-GPI and PLAP were previously obtained (Paladino et al., 2004). In particular, the GFP-GPI construct previously used by us and others (Nichols et al., 2001; Paladino et al., 2004; Polishchuk et al., 2004) was a gift from S. Lacey (Southwestern University, Georgetown, TX). The fusion was constructed in the eukaryotic expression vector pJB20. It has an EcoRI site at the 5′ end, a HindIII site at the 3′ end, and a PstI site that separates the ecto- and anchor domain. TER was measured using a meter (Millicell-ERS; Millipore).

Fluorescence microscopy

Unless specifically indicated, MDCK cells were grown on Transwell filters for 3.5–4 d, washed with PBS containing $CaCl_2$ and $MgCl_2$, fixed with 4% PFA, and quenched with 50 mM NH_4Cl. Depending on the experiment, cells were permeabilized with 0.075% saponin. Primary antibodies were detected with FITC or TRITC-conjugated secondary antibodies. Images were collected using a laser scanning confocal microscope (LSM 510; Carl Zeiss MicroImaging, Inc.) equipped with a plan Apo 63× NA 1.4 oil immersion objective lens (Carl Zeiss MicroImaging, Inc.). As previously described (Nichols et al., 2001), the quantification of mean fluorescence intensities in selected regions of interest were performed using a laser scanning microscope (LSM 510; Carl Zeiss MicroImaging, Inc.). In particular, the fluorescence intensities of areas of equal size in a single z plane through the cell monolayer (from a range of 1–3, 4–6, and 8–12 μm starting from the top of the cell for apical, Golgi, and basolateral signals, respectively) were measured and corrected for background.

Time-lapse images were collected using a confocal microscopy system (UltraView ERS; PerkinElmer) equipped with a microscope (Axiovert 200; Carl Zeiss MicroImaging, Inc.). A plan Apo 63× or a 100× NA 1.4 oil immersion objective lens was controlled by a piezoelectric z stepper. To image living cells, we mounted the filter on an optical glass in a petri dish containing CO_2 independent medium (150 mM NaCl, 5 mM KCl, 1 mM $CaCl_2$, 1 mM $MgCl_2$, and 20 mM Hepes, pH 7.4). Cells were imaged using a thermostatic chamber mounted on the microscope set at 37°C. Cells were imaged every 3 min for a total of 50–60 min or every 1 min for 10–15 min, collecting 15 or 20 z slices (confocal depth of 0.5 μm) each time. For short time lapses (3–5 min), cells were imaged every 2 s, collecting four to six z slices (confocal depth of 1 μm) at high magnification using a plan Apo 100× NA 1.4 oil immersion objective lens and an optovar 1.6× lens. Images and videos were volume rendered by Volocity software (PerkinElmer).

Targeting assays

Labeling assay. Cells grown on filter were starved of methionine for 1 h and pulse labeled for 15 min with medium containing 100 μCi/ml [^{35}S]methionine (GE Healthcare) and incubated in chase medium (DME containing 5% FBS and 10× methionine) for different times. At the end of each chase time, cells were selectively biotinylated and processed as described in the supplemental material (available at http://www.jcb.org/cgi/content/full/jcb.200507116/DC1). Lysates were immunoprecipitated with specific antibodies, and biotinylated antigens were then precipitated with streptavidin beads. Samples were run on SDS-PAGE and analyzed by a phosphorimager. Quantifications were performed by ImageQuant (GE Healthcare).

Cold assay. Cells grown on filter were incubated with 25 μg/ml trypsin in DME without serum for 30 min twice. They were then subjected to temperature block as described below and warmed at 37°C for different times in culture medium containing 150 μg/ml cycloheximide. At the end of each time point, surface proteins were selectively biotinylated, immunoprecipitated with an antibody against GFP, and run on SDS-PAGE. Biotinylated proteins were revealed by HRP-conjugated streptavidin. Quantifications were performed with Image software (National Institutes of Health).

Temperature block

To achieve an almost complete protein block in the TGN, we used a previously published protocol (Paladino et al., 2004). Filter-grown cells were incubated at 19.5°C for 2 h in areal medium (F12 Coon's modified medium without $NaHCO_3$ and with 0.2% BSA and 20 mM Hepes, pH 7.4). In the last hour at 19.5°C, they were treated with 150 μg/ml cycloheximide.

Permeability assay

1 μCi [^{14}C]inulin (MP Biomedicals) diluted in 500 μl DME was added to the apical chamber of the Transwell filters, and cells were incubated for 30 or 60 min at 37°C. The amount of [^{14}C]inulin that remained in the apical well, traversed the filter to the basal well, or remained cell associated was quantified in a liquid scintillation counter.

Online supplemental material

Fig. S1 shows pulse chase and biotinylation targeting assays. In fully polarized cells (A), NTR-PLAP is directly targeted to the apical surface, whereas it undergoes transcytosis in unpolarized cells. In not fully polarized cells (B), a portion of GFP-GPI can be indirectly sorted to the apical membrane. Fig. S2 shows by immunofluorescence (A) and Western blotting (B) that trypsin is a suitable tool to remove GFP-GPI without impairing the integrity of the cell monolayer. Fig. S3 shows that tannic acid impairs transferrin internalization but does not affect surface binding. Fig. S4 A shows that apical and basolateral markers are correctly localized in cells grown on filters upside down, indicating that cells are well polarized. It also shows that YFP-PIT is basolaterally localized, and it is partially segregated from CFP-GPI at the TGN and is in different post-TGN carriers (B and C, respectively). Fig. S5 shows that ∼6–8% of GFP-GPI is slowly internalized from the basolateral surface. Videos 1–9 show the arrival of GFP-GPI from the TGN to the plasma membrane. They clearly show the direct appearance of GFP-GPI fluorescence at the apical surface both in control and tannic acid–treated cells. All z planes were volume rendered by Volocity software. Online supplemental material is available at http://www.jcb.org/cgi/content/full/jcb.200507116/DC1.

We thank Dr. Chris Bowler for critical reading of the manuscript, Dr. A. le Bivic for helpful discussions, and Dr. C. Blackmore (PerkinElmer) for help in image processing.

This work was supported by grants to C. Zurzolo from the Ministero dell'Università e della Ricerca Scientifica e Tecnologica, Programmi a Cofinanziamento Programmi di Ricerca di Interesse Nazionale 2004, Fondo per gli Investimenti della Ricerca di Base 2003, and the European Union (HPRN_CT_2000_00077).

Submitted: 22 July 2005
Accepted: 13 December 2005

References

Ang, A.L., T. Taguchi, S. Francis, H. Folsch, L.J. Murrells, M. Pypaert, G. Warren, and I. Mellman. 2004. Recycling endosomes can serve as intermediates during transport from the Golgi to the plasma membrane of MDCK cells. *J. Cell Biol.* 167:531–543.

Apodaca, G., and K.E. Mostov. 1993. Transcytosis of placental alkaline phosphatase-polymeric immunoglobulin receptor fusion proteins is regulated by mutations of Ser664. *J. Biol. Chem.* 268:23712–23719.

Apodaca, G., M. Bomsel, R. Lindstedt, J. Engel, D. Frank, K.E. Mostov, and J. Wiener-Kronish. 1995. Characterization of *Pseudomonas aeruginosa*-induced MDCK cell injury: glycosylation-defective host cells are resistant to bacterial killing. *Infect. Immun.* 63:1541–1551.

Arreaza, G., and D.A. Brown. 1995. Sorting and intracellular trafficking of a glycosylphosphatidylinositol-anchored protein and two hybrid transmembrane proteins with the same ectodomain in Madin-Darby canine kidney epithelial cells. *J. Biol. Chem.* 270:23641–23647.

Bonifacino, J.S., and L.M. Traub. 2003. Signals for sorting of transmembrane proteins to endosomes and lysosomes. *Annu. Rev. Biochem.* 72:395–447.

Brown, D.A., and J.K. Rose. 1992. Sorting of GPI-anchored proteins to glycolipid-enriched membrane subdomains during transport to the apical cell surface. *Cell*. 68:533–544.

Casanova, J.E., P.P. Breitfeld, S.A. Ross, and K.E. Mostov. 1990. Phosphorylation of the polymeric immunoglobulin receptor required for its efficient transcytosis. *Science*. 248:742–745.

Chatterjee, S., E.R. Smith, K. Hanada, V.L. Stevens, and S. Mayor. 2001. GPI anchoring leads to sphingolipid-dependent retention of endocytosed proteins in the recycling endosomal compartment. *EMBO J.* 20:1583–1592.

Chuang, J.Z., and C.H. Sung. 1998. The cytoplasmic tail of rhodopsin acts as a novel apical sorting signal in polarized MDCK cells. *J. Cell Biol.* 142:1245–1256.

Folsch, H., H. Ohno, J.S. Bonifacino, and I. Mellman. 1999. A novel clathrin adaptor complex mediates basolateral targeting in polarized epithelial cells. *Cell*. 99:189–198.

Folsch, H., M. Pypaert, S. Maday, L. Pelletier, and I. Mellman. 2003. The AP-1A and AP-1B clathrin adaptor complexes define biochemically and functionally distinct membrane domains. *J. Cell Biol.* 163:351–362.

Gottardi, C.J., and M.J. Caplan. 1993. Delivery of Na+,K(+)-ATPase in polarized epithelial cells. *Science*. 260:552–554.

Griffiths, G., and K. Simons. 1986. The trans Golgi network: sorting at the exit site of the Golgi complex. *Science*. 234:438–443.

Inouye, S., and F.I. Tsuji. 1994. Aequorea green fluorescent protein. Expression of the gene and fluorescence characteristics of the recombinant protein. *FEBS Lett.* 341:277–280.

Jacob, R., and H.Y. Naim. 2001. Apical membrane proteins are transported in distinct vesicular carriers. *Curr. Biol.* 11:1444–1450.

Jacob, R., M. Heine, M. Alfalah, and H.Y. Naim. 2003. Distinct cytoskeletal tracks direct individual vesicle populations to the apical membrane of epithelial cells. *Curr. Biol.* 13:607–612.

Keller, G.A., M.W. Siegel, and I.W. Caras. 1992. Endocytosis of glycophospholipid-anchored and transmembrane forms of CD4 by different endocytic pathways. *EMBO J.* 11:863–874.

Keller, P., D. Toomre, E. Diaz, J. White, and K. Simons. 2001. Multicolour imaging of post-Golgi sorting and trafficking in live cells. *Nat. Cell Biol.* 3:140–149.

Kreitzer, G., J. Schmoranzer, S.H. Low, X. Li, Y. Gan, T. Weimbs, S.M. Simon, and E. Rodriguez-Boulan. 2003. Three-dimensional analysis of post-Golgi carrier exocytosis in epithelial cells. *Nat. Cell Biol.* 5:126–136.

Lemmers, C., E. Medina, M.H. Delgrossi, D. Michel, J.P. Arsanto, and A. Le Bivic. 2002. hINADl/PATJ, a homolog of discs lost, interacts with crumbs and localizes to tight junctions in human epithelial cells. *J. Biol. Chem.* 277:25408–25415.

Lipardi, C., L. Nitsch, and C. Zurzolo. 2000. Detergent-insoluble GPI-anchored proteins are apically sorted in fischer rat thyroid cells, but interference with cholesterol or sphingolipids differentially affects detergent insolubility and apical sorting. *Mol. Biol. Cell*. 11:531–542.

Lisanti, M.P., I.W. Caras, T. Gilbert, D. Hanzel, and E. Rodriguez-Boulan. 1990. Vectorial apical delivery and slow endocytosis of a glycolipid-anchored fusion protein in transfected MDCK cells. *Proc. Natl. Acad. Sci. USA*. 87:7419–7423.

Luo, W., and A. Chang. 2000. An endosome-to-plasma membrane pathway involved in trafficking of a mutant plasma membrane ATPase in yeast. *Mol. Biol. Cell*. 11:579–592.

Marmorstein, A.D., K.G. Csaky, J. Baffi, L. Lam, F. Rahaal, and E. Rodriguez-Boulan. 2000. Saturation of, and competition for entry into, the apical secretory pathway. *Proc. Natl. Acad. Sci. USA*. 97:3248–3253.

Matter, K. 2000. Epithelial polarity: sorting out the sorters. *Curr. Biol.* 10:R39–R42.

Matter, K., and M.S. Balda. 2003. Functional analysis of tight junctions. *Methods*. 30:228–234.

Mayor, S., and H. Riezman. 2004. Sorting GPI-anchored proteins. *Nat. Rev. Mol. Cell Biol.* 5:110–120.

Mellman, I. 1996. Endocytosis and molecular sorting. *Annu. Rev. Cell Dev. Biol.* 12:575–625.

Monlauzeur, L., L. Breuza, and A. Le Bivic. 1998. Putative O-glycosylation sites and a membrane anchor are necessary for apical delivery of the human neurotrophin receptor in Caco-2 cells. *J. Biol. Chem.* 273:30263–30270.

Mostov, K.E., A. de Bruyn Kops, and D.L. Deitcher. 1986. Deletion of the cytoplasmic domain of the polymeric immunoglobulin receptor prevents basolateral localization and endocytosis. *Cell*. 47:359–364.

Mostov, K.E., M. Verges, and Y. Altschuler. 2000. Membrane traffic in polarized epithelial cells. *Curr. Opin. Cell Biol.* 12:483–490.

Newman, T.M., M. Tian, and B.D. Gomperts. 1996. Ultrastructural characterization of tannic acid-arrested degranulation of permeabilized guinea pig eosinophils stimulated with GTP-gamma-S. *Eur. J. Cell Biol.* 70:209–220.

Nichols, B.J., A.K. Kenworthy, R.S. Polishchuk, R. Lodge, T.H. Roberts, K. Hirschberg, R.D. Phair, and J. Lippincott-Schwartz. 2001. Rapid cycling of lipid raft markers between the cell surface and Golgi complex. *J. Cell Biol.* 153:529–541.

Paladino, S., D. Sarnataro, R. Pillich, S. Tivodar, L. Nitsch, and C. Zurzolo. 2004. Protein oligomerization modulates raft partitioning and apical sorting of GPI-anchored proteins. *J. Cell Biol.* 167:699–709.

Polishchuk, R., A. Di Pentima, and J. Lippincott-Schwartz. 2004. Delivery of raft-associated, GPI-anchored proteins to the apical surface of polarized MDCK cells by a transcytotic pathway. *Nat. Cell Biol*. 6:297–307.

Rodriguez-Boulan, E., G. Kreitzer, and A. Musch. 2005. Organization of vesicular trafficking in epithelia. *Nat. Rev. Mol. Cell Biol.* 6:233–247.

Sarnataro, D., L. Nitsch, W. Hunziker, and C. Zurzolo. 2000. Detergent insoluble microdomains are not involved in transcytosis of polymeric Ig receptor in FRT and MDCK cells. *Traffic*. 1:794–802.

Scheiffele, P., J. Peranen, and K. Simons. 1995. N-glycans as apical sorting signals in epithelial cells. *Nature*. 378:96–98.

Scheiffele, P., M.G. Roth, and K. Simons. 1997. Interaction of influenza virus haemagglutinin with sphingolipid-cholesterol membrane domains via its transmembrane domain. *EMBO J.* 16:5501–5508.

Schell, M.J., M. Maurice, B. Stieger, and A.L. Hubbard. 1992. 5′nucleotidase is sorted to the apical domain of hepatocytes via an indirect route. *J. Cell Biol.* 119:1173–1182.

Shin, K., S. Straight, and B. Margolis. 2005. PATJ regulates tight junction formation and polarity in mammalian epithelial cells. *J. Cell Biol.* 168:705–711.

Simons, K., and E. Ikonen. 1997. Functional rafts in cell membranes. *Nature*. 387:569–572.

Song, W., G. Apodaca, and K. Mostov. 1994. Transcytosis of the polymeric immunoglobulin receptor is regulated in multiple intracellular compartments. *J. Biol. Chem.* 269:29474–29480.

Sugimoto, H., M. Sugahara, H. Folsch, Y. Koide, F. Nakatsu, N. Tanaka, T. Nishimura, M. Furukawa, C. Mullins, N. Nakamura, et al. 2002. Differential recognition of tyrosine-based basolateral signals by AP-1B subunit mu1B in polarized epithelial cells. *Mol. Biol. Cell*. 13:2374–2382.

Sun, A.Q., M. Ananthanarayanan, C.J. Soroka, S. Thevananther, B.L. Shneider, and F.J. Suchy. 1998. Sorting of rat liver and ileal sodium-dependent bile acid transporters in polarized epithelial cells. *Am. J. Physiol.* 275:G1045–G1055.

Wandinger-Ness, A., M.K. Bennett, C. Antony, and K. Simons. 1990. Distinct transport vesicles mediate the delivery of plasma membrane proteins to the apical and basolateral domains of MDCK cells. *J. Cell Biol.* 111:987–1000.

Zurzolo, C., and E. Rodriguez-Boulan. 1993. Delivery of Na+,K(+)-ATPase in polarized epithelial cells. *Science*. 260:550–552.

Zurzolo, C., A. Le Bivic, A. Quaroni, L. Nitsch, and E. Rodriguez-Boulan. 1992. Modulation of transcytotic and direct targeting pathways in a polarized thyroid cell line. *EMBO J.* 11:2337–2344.